Supplementary Information for

Evidence for mass independent fractionation of even mercury isotopes in the troposphere

Shuyuan Huang[1,2], Yunlong Huo[1], Heng Sun[1], Supeng Lv[1], Yuhan Zhao[1,2], Kunning Lin[1], Yaojin Chen[2], Yuanbiao Zhang[1*]

[1]*Third Institute of Oceanography, Ministry of Natural Resources, Xiamen, Fujian 361005, China*

[2]*State Key Laboratory of Marine Environmental Science, Xiamen University, Xiamen, Fujian 361102, China*

*Correspondence to:
Yuanbiao Zhang (zhangyuanbiao@tio.org.cn)

Supplementary Notes

Note S1: Details on preconcentration

Dual-stage tube furnace with solution-trapping systems were installed following previous study [1]. Quartz fiber membranes with the collected PBM was individually installed in the first tube furnace and combusted to 1000°C within 3.0 h and maintained for 1.0 h. The second tube furnace was programmed to maintain at 1000°C during sample processing. 5 mL $KMnO_4$ trapping solution (0.1%$KMnO_4$ (*m/v*) + 10% H_2SO_4 (*v/v*)) was utilized to capture the Hg vapor, which was released from the vent of the furnace. One trapping solution was used for preconcentration of 2-4 membranes. The Hg concentrations in the trapping solutions were measured by CVAFS following USEPA Method 1631.

Note S2. Details on calculation of Hg isotopic compositions of PBM

In order to obtain Hg isotopic compositions of PBM in MBL at higher resolution (2-4 days), isotope binary mixing model was applied for determination of Hg isotopic compositions in PBM samples with low Hg concentration, following our previous study [2]. In this study, the Hg concentrations of trapping solutions were lower than 1.0 ng/L. 50 μL 50 ng/mL Hg standard solutions (NIST 3133) were added to the trapping solutions to ensure sufficient Hg mass (approximately 5 ng) for isotope analysis. The Hg isotopic compositions of PBM could be calculated by the following equations:

$$\delta^{xxx}Hg_{PBM} = \delta^{xxx}Hg_{Mix}/X_{PBM} \quad (1)$$

$$\Delta^{xxx}Hg_{PBM} = \Delta^{xxx}Hg_{Mix}/X_{PBM} \quad (2)$$

$$X_{PBM} = m_{PBM}/(m_{PBM}+m_{3133}) \quad (3)$$

where xxx values are 199, 200, 201, and 202 amu, Mix denote mixing solution contains trapping solution and Hg standard solution, X_{Sam} are the Hg mass fractions of the PBM in the mixing solution. The m_{PBM} and m_{3133} are the Hg mass of PBM and NIST 3133 in the mixing solution, respectively. The Hg mass of PBM could be calculated through Hg concentrations of trapping solutions, while Hg mass of NIST 3133 was 2.5 ng.

The uncertainties associated with equations (1) and (2) could be estimated by the following equation:

$$\sigma_{PBM} = \sqrt{\frac{1}{X_{PBM}^2} \times \sigma_{Mix}^2 + \frac{d_{Mix}^2}{X_{PBM}^4} \times \sigma_X^2} \quad (4)$$

where σ_{PBM} and σ_X represent the 2SD values of the mixing solution and mass fractions, respectively, and d_{Mix} represents both the MDF and MIF values (including $\delta^{202}Hg$, $\Delta^{199}Hg$, $\Delta^{200}Hg$, and $\Delta^{201}Hg$) of the mixing solutions. The results were listed in Supplementary Table 1.

Table S1 Hg isotopic compositions of the standards and solution samples

ID	Hg (ng/mL)	n	δ^{202}Hg (‰)	2SD	Δ^{199}Hg (‰)	2SD	Δ^{200}Hg (‰)	2SD	Δ^{201}Hg (‰)	2SD
standards										
NIST 3133	3.0	12	-0.01	0.06	0	0.02	0	0.02	-0.01	0.02
NIST 3133	1.0	6	-0.04	0.08	0.01	0.04	-0.01	0.04	0.02	0.06
NIST 8610	1.0	5	-0.52	0.12	-0.02	0.04	0.00	0.02	-0.05	0.05
samples										
1	0.81	1	-0.06	0.12	-0.15	0.04	0.15	0.02	-0.18	0.05
2	0.96	1	-0.50	0.12	-0.01	0.04	0.03	0.02	0.02	0.05
3	0.76	1	-0.24	0.12	-0.06	0.04	0.08	0.02	-0.07	0.05
4	0.95	1	-0.36	0.12	0.17	0.04	0.00	0.02	0.13	0.05
5	0.80	1	-0.22	0.12	0.11	0.04	0.09	0.02	0.13	0.05
6	0.89	1	-0.59	0.12	0.11	0.04	0.11	0.02	0.05	0.05
7	0.77	1	-0.75	0.12	0.07	0.04	0.15	0.02	0.12	0.05
8	1.10	1	-0.02	0.12	0.13	0.04	0.01	0.02	0.06	0.05
9	0.93	1	-0.33	0.12	0.04	0.04	-0.03	0.02	0.03	0.05
10	0.93	1	-0.21	0.12	0.10	0.04	0.06	0.02	0.12	0.05
11	1.01	1	-0.04	0.12	-0.01	0.04	0.06	0.02	-0.01	0.05
12	0.82	1	-0.46	0.12	-0.12	0.04	0.16	0.02	-0.13	0.05
13	0.81	1	-0.05	0.12	0.08	0.04	-0.02	0.02	0.08	0.05
14	0.90	1	-0.83	0.12	0.16	0.04	0.08	0.02	0.15	0.05

15	0.92	1	-0.87	0.12	0.03	0.04	0.07	0.02	0.08	0.05
16	0.85	1	-1.05	0.12	-0.12	0.04	-0.01	0.02	-0.08	0.05
17	0.95	1	-1.01	0.12	-0.08	0.04	0.09	0.02	-0.04	0.05
18	0.80	1	-0.81	0.12	-0.09	0.04	0.10	0.02	-0.09	0.05
19	0.85	1	-0.93	0.12	0.18	0.04	0.07	0.02	0.17	0.05
20	0.87	1	-0.30	0.12	0.17	0.04	0.11	0.02	0.16	0.05
21	1.03	1	-1.25	0.12	0.05	0.04	0.07	0.02	0.00	0.05
22	0.93	1	-0.33	0.12	0.13	0.04	0.04	0.02	0.12	0.05
23	0.77	1	0.11	0.12	0.23	0.04	0.11	0.02	0.20	0.05
24	0.75	1	-0.22	0.12	0.15	0.04	-0.02	0.02	0.12	0.05
25	0.94	1	-0.66	0.12	-0.13	0.04	0.00	0.02	-0.08	0.05
26	0.95	1	-0.35	0.12	-0.15	0.04	-0.05	0.02	-0.17	0.05
27	0.90	1	-0.27	0.12	0.06	0.04	-0.05	0.02	0.14	0.05
28	0.84	1	-0.09	0.12	0.00	0.04	0.10	0.02	-0.03	0.05
29	0.71	1	-0.34	0.12	-0.04	0.04	0.09	0.02	-0.03	0.05
30	0.82	1	-0.35	0.12	0.07	0.04	0.06	0.02	0.01	0.05
31	0.80	1	-0.35	0.12	0.12	0.04	0.03	0.02	0.17	0.05
32	0.76	1	-0.36	0.12	0.17	0.04	0.13	0.02	0.19	0.05
33	0.97	1	-0.72	0.12	-0.03	0.04	0.00	0.02	-0.03	0.05
34	0.76	1	-0.24	0.12	0.05	0.04	0.14	0.02	0.01	0.05
35	0.80	1	-0.18	0.12	0.07	0.04	0.12	0.02	0.10	0.05
36	0.98	1	-0.14	0.12	0.16	0.04	0.12	0.02	0.11	0.05
37	0.78	1	-0.27	0.12	-0.11	0.04	-0.04	0.02	-0.13	0.05
38	0.99	1	-0.36	0.12	-0.04	0.04	0.06	0.02	-0.04	0.05
39	0.85	1	-0.38	0.12	0.07	0.04	0.06	0.02	0.02	0.05
40	0.86	1	-0.40	0.12	-0.21	0.04	0.06	0.02	-0.18	0.05

41	0.75	1	0.13	0.12	0.10	0.04	0.02	0.02	0.06	0.05
42	0.78	1	-0.48	0.12	0.06	0.04	0.11	0.02	0.08	0.05
43	0.84	1	-0.22	0.12	0.12	0.04	0.09	0.02	0.08	0.05
44	1.16	1	-0.68	0.12	0.20	0.04	0.04	0.02	0.16	0.05
45	0.74	1	-0.24	0.12	0.15	0.04	0.01	0.02	0.14	0.05
46	0.81	1	-0.30	0.12	-0.11	0.04	0.12	0.02	-0.12	0.05
47	1.16	1	-1.13	0.12	-0.05	0.04	-0.01	0.02	-0.02	0.05
48	1.52	1	-0.85	0.12	-0.06	0.04	0.04	0.02	-0.03	0.05
49	0.96	1	-0.38	0.12	-0.05	0.04	0.04	0.02	-0.02	0.05
50	1.38	1	-1.20	0.12	0.14	0.04	0.02	0.02	0.11	0.05
51	1.04	1	-0.89	0.12	0.15	0.04	0.02	0.02	0.10	0.05
52	0.80	1	0.21	0.12	-0.14	0.04	0.10	0.02	-0.07	0.05

Table S2. Sampling information of PBM samples and their calculated isotopic compositions as illustrated in Supplementary Note 2

ID	Sampling period	Longitude (°E)	Latitude (°N)	V (m^3)	PBM (pg/m^3)	X_{Sam}	$\delta^{202}Hg$ (‰)	2SD	$\Delta^{199}Hg$ (‰)	2SD	$\Delta^{200}Hg$ (‰)	2SD	$\Delta^{201}Hg$ (‰)	2SD
Cruise A														
1	20190814-20190816	123.21	21.41	108.14	14.4	0.38	-0.15	0.31	-0.39	0.11	0.39	0.06	-0.46	0.14
2	20190816-20190818	129.25	21.89	103.26	22.3	0.48	-1.04	0.26	-0.03	0.08	0.07	0.04	0.04	0.10
3	20190818-20190820	135.46	22.99	100.02	13.2	0.35	-0.70	0.35	-0.18	0.12	0.24	0.06	-0.20	0.15
4	20190820-20190822	143.76	24.09	102.20	22.3	0.48	-0.76	0.26	0.35	0.09	0.00	0.04	0.28	0.11
5	20190822-20190824	151.55	24.74	102.24	14.5	0.37	-0.60	0.33	0.30	0.11	0.24	0.06	0.35	0.14
6	20190824-20190826	156.50	23.97	106.15	18.2	0.44	-1.35	0.29	0.25	0.09	0.25	0.05	0.11	0.11
7	20190826-20190828	157.96	20.56	108.78	12.6	0.35	-2.12	0.38	0.19	0.11	0.42	0.07	0.34	0.14
8	20190828-20190901	160.25	15.17	142.38	21.1	0.55	-0.03	0.22	0.23	0.07	0.02	0.04	0.11	0.09
9	20190904-20190908	167.99	19.50	149.40	14.5	0.46	-0.71	0.26	0.08	0.09	-0.07	0.04	0.06	0.11
10	20190910-20190912	175.46	16.44	201.40	10.6	0.46	-0.45	0.26	0.22	0.09	0.13	0.04	0.26	0.11
11	20190912-20190915	179.99	17.80	160.51	15.9	0.51	-0.08	0.24	-0.03	0.08	0.13	0.04	-0.02	0.10
12	20190915-20190917	179.99	22.79	104.54	15.2	0.39	-1.19	0.32	-0.32	0.11	0.42	0.06	-0.34	0.13
13	20190917-20190920	177.49	24.00	136.12	11.4	0.38	-0.13	0.31	0.20	0.11	-0.04	0.05	0.20	0.13
14	20190920-20190922	174.99	20.98	110.97	17.8	0.44	-1.87	0.30	0.37	0.09	0.19	0.05	0.34	0.12
15	20190922-20190924	174.93	16.95	112.86	18.7	0.46	-1.90	0.29	0.06	0.09	0.14	0.04	0.17	0.11
16	20190924-20190926	170.65	13.64	102.58	17.2	0.41	-2.53	0.34	-0.30	0.10	-0.02	0.05	-0.19	0.12
17	20190926-20190929	158.65	7.33	157.06	14.3	0.47	-2.15	0.29	-0.16	0.09	0.19	0.04	-0.08	0.11
18	20190929-20191002	158.20	7.00	173.33	8.8	0.38	-2.15	0.36	-0.23	0.11	0.26	0.06	-0.24	0.13
19	20191002-20191004	162.49	9.78	103.78	16.7	0.41	-2.28	0.34	0.45	0.10	0.17	0.05	0.42	0.13
20	20191004-20191006	170.58	13.97	106.49	17.3	0.42	-0.70	0.29	0.40	0.10	0.27	0.05	0.38	0.12
21	20191006-20191008	178.02	16.69	111.56	24.0	0.52	-2.42	0.27	0.09	0.08	0.13	0.04	0.00	0.10

22	20191008-20191010	-174.14	19.23	110.40	19.5	0.46	-0.70	0.26	0.28	0.09	0.08	0.04	0.26	0.11
23	20191010-20191012	-165.97	20.50	110.35	12.3	0.35	0.32	0.34	0.67	0.13	0.31	0.06	0.56	0.15
24	20191012-20191015	-166.01	20.50	159.57	8.0	0.34	-0.64	0.36	0.44	0.12	-0.06	0.06	0.36	0.15
25	20191015-20191017	-173.01	20.50	87.93	25.3	0.47	-1.41	0.27	-0.27	0.09	-0.01	0.04	-0.17	0.11
26	20191017-20191019	179.99	20.49	105.13	21.3	0.47	-0.74	0.26	-0.32	0.09	-0.10	0.04	-0.36	0.11
27	20191020-20191023	172.93	21.25	183.12	11.0	0.45	-0.60	0.27	0.12	0.09	-0.11	0.05	0.31	0.11
28	20191023-20191025	169.99	23.51	107.13	15.8	0.40	-0.22	0.30	0.01	0.10	0.24	0.05	-0.07	0.12
29	20191025-20191026	166.85	23.47	66.58	16.1	0.30	-1.14	0.42	-0.15	0.13	0.29	0.07	-0.09	0.17
30	20191026-20191029	160.73	21.23	156.56	10.3	0.39	-0.88	0.31	0.18	0.10	0.14	0.05	0.03	0.13
31	20191029-20191031	153.24	20.76	110.55	13.6	0.37	-0.95	0.33	0.33	0.11	0.09	0.05	0.45	0.14
32	20191031-20191102	143.82	21.28	110.06	12.0	0.35	-1.03	0.36	0.50	0.12	0.37	0.07	0.55	0.15
33	20191102-20191104	133.26	22.13	95.28	24.8	0.49	-1.47	0.26	-0.07	0.08	0.00	0.04	-0.06	0.10
Cruise B														
34	20180514-20180516	134.63	21.00	144.00	8.9	0.34	-0.71	0.36	0.15	0.12	0.40	0.07	0.02	0.15
35	20180516-20180520	146.49	23.50	98.00	15.4	0.38	-0.48	0.32	0.19	0.11	0.32	0.06	0.27	0.13
36	20180520-20180523	146.50	28.50	144.00	16.7	0.49	-0.29	0.25	0.33	0.08	0.24	0.04	0.22	0.10
37	20180523-20180525	146.55	33.02	94.93	14.6	0.36	-0.75	0.34	-0.31	0.12	-0.11	0.06	-0.35	0.14
38	20180525-20180527	146.55	37.02	95.85	25.7	0.50	-0.73	0.25	-0.08	0.08	0.11	0.04	-0.08	0.10
39	20180527-20180529	149.24	37.00	96.23	18.1	0.41	-0.92	0.30	0.16	0.10	0.15	0.05	0.05	0.12
40	20180529-20180604	139.72	30.36	144.00	12.4	0.42	-0.95	0.30	-0.50	0.10	0.15	0.05	-0.43	0.12
Cruise C														
41	20190813-20190815	123.15	34.52	110.59	11.5	0.34	0.39	0.36	0.30	0.12	0.07	0.06	0.18	0.15
42	20190815-20190817	129.83	35.72	110.59	12.7	0.36	-1.34	0.35	0.16	0.11	0.31	0.06	0.22	0.14
43	20190817-20190819	137.46	42.12	58.75	29.1	0.41	-0.55	0.30	0.30	0.10	0.23	0.05	0.19	0.12
44	20190819-20190821	147.31	47.73	83.38	39.6	0.57	-1.19	0.22	0.35	0.07	0.06	0.04	0.28	0.09
45	20190821-20190823	158.35	50.97	84.67	14.0	0.32	-0.76	0.38	0.48	0.13	0.02	0.06	0.43	0.16

46	20190823-20190825	168.99	54.44	49.68	31.1	0.38	-0.78	0.32	-0.28	0.11	0.32	0.06	-0.31	0.13
47	20190825-20190827	176.53	57.67	51.84	63.4	0.57	-1.99	0.24	-0.09	0.07	-0.02	0.04	-0.04	0.09
48	20190827-20190829	-176.79	61.36	103.68	49.2	0.67	-1.27	0.19	-0.09	0.06	0.06	0.03	-0.04	0.07
49	20190829-20190831	-170.37	67.32	51.84	44.2	0.48	-0.78	0.26	-0.11	0.08	0.09	0.04	-0.04	0.10
50	20190831-20190902	-170.39	73.34	103.68	42.6	0.64	-1.88	0.21	0.22	0.06	0.03	0.03	0.17	0.08
51	20190902-20190905	-170.49	71.88	103.68	25.9	0.52	-1.71	0.25	0.29	0.08	0.04	0.04	0.19	0.10
52	20190905-20190909	-169.23	64.78	82.08	18.0	0.37	0.57	0.33	-0.38	0.11	0.27	0.06	-0.18	0.14

Table S3 Parameter settings in HYSPLIT model

Parameters	Values
Number of Trajectory Starting Locations	1
Type of Trajectory	Frequency
Trajectory Direction	Backward
Vertical Motion	Model vertical velocity
Total run time (h)	120 (48)*
Number of days to calculate trajectory frequencies (d)	5 (2)*
Trajectory frequency grid resolution (deg.)	0.50
Trajectory starting interval (h)	3
Height (meters AGL)	500
Plot resolution (dpi)	96
Zoom factor	70

Table S4. Frequencies of height of backward trajectories of air mass

ID	f_{3000} (%)	f_{1500} (%)	f_{500} (%)	f_{3000_light} (%)	f_{1500_light} (%)	f_{500_light} (%)
1	5.27	20.78	28.06	3.06	12.24	17.30
2	10.13	19.73	35.23	5.91	11.81	21.10
3	0.00	0.00	6.65	0.00	0.00	4.01
4	2.00	14.56	23.63	1.27	8.76	13.71
5	0.00	0.42	18.57	0.00	0.11	10.65
6	0.00	0.42	35.97	0.00	0.00	21.10
7	0.00	10.34	29.22	0.00	5.91	16.56
8	0.00	0.21	17.19	0.00	0.00	10.13
9	2.64	18.99	35.02	1.48	11.08	20.25
10	0.00	0.00	11.60	0.00	0.00	6.33
11	0.00	0.00	10.97	0.00	0.00	6.43
12	9.05	24.37	44.83	5.43	13.92	26.16
13	6.82	28.80	48.42	3.83	16.35	28.59
14	1.60	6.86	13.40	1.17	4.43	8.33
15	0.00	0.00	14.98	0.00	0.00	9.39
16	0.00	0.00	10.55	0.00	0.00	6.33
17	0.00	8.86	14.03	0.00	5.38	8.33
18	0.00	0.00	0.00	0.00	0.00	0.00
19	0.00	0.00	0.00	0.00	0.00	0.00
20	0.00	0.00	5.27	0.00	0.00	2.53
21	2.74	18.67	34.07	1.90	10.55	19.41
22	4.22	13.19	36.60	2.64	7.28	22.26
23	11.18	16.35	32.07	6.01	9.39	19.09
24	23.52	39.14	57.17	13.40	22.47	32.81
25	15.82	42.62	55.70	8.86	25.21	32.38
26	4.43	32.91	51.79	2.11	19.09	30.27
27	0.00	3.59	22.26	0.00	2.43	12.55
28	4.64	8.97	21.73	2.85	5.17	11.71
29	4.43	10.86	32.81	2.53	6.01	19.62
30	4.43	13.08	24.89	2.64	7.81	15.19
31	3.27	7.59	17.62	1.48	4.32	10.02
32	0.00	8.44	32.38	0.00	4.01	18.46
33	0.00	6.65	13.29	0.00	3.48	7.49
34	0.00	0.00	18.25	0.00	0.00	13.08
35	0.00	0.00	0.00	0.00	0.00	0.00
36	0.00	30.38	46.73	0.00	21.52	33.44
37	8.65	29.11	52.22	5.91	20.78	36.60
38	18.04	34.60	46.31	12.55	24.05	32.38
39	22.78	31.86	50.32	15.82	22.05	35.44
40	29.64	34.81	50.11	20.78	24.26	35.34
41	37.97	68.46	84.49	26.79	47.36	59.60
42	16.35	52.64	75.11	11.50	36.39	53.16
43	18.04	48.52	69.51	12.66	34.60	49.47
44	11.18	28.16	65.93	8.02	20.25	46.10
45	0.00	33.12	66.24	0.00	26.16	52.11
46	0.00	29.54	56.22	0.00	23.21	43.57
47	0.00	10.76	59.39	0.00	8.02	46.31
48	4.01	22.78	48.63	2.53	17.51	37.55
49	3.48	23.73	53.27	3.48	23.73	53.27
50	0.00	10.55	27.64	0.00	10.55	27.64
51	0.00	0.00	10.76	0.00	0.00	10.76
52	16.24	27.22	32.49	16.24	27.22	32.49

Table S5. The isotopic compositions of three end-members of troposphere photochemical reactions, GEM oxidation, and photoreduction.

Sample ID	Δ^{199}Hg (‰)	2SD	Δ^{200}Hg (‰)	2SD	references
PBM samples dominated by GEM oxidation					
GKD41	-0.37	0.08	0.00	0.07	
GKD351	-0.58	0.08	0.05	0.07	3
GKD353	-0.85	0.08	0.03	0.07	
GKD355	-0.80	0.08	0.01	0.07	
AE-TPM-03	-0.33	0.07	0.06	0.06	
AE-TPM-04	-0.41	0.07	0.08	0.06	
AE-TPM-05	-0.38	0.07	0	0.06	
AE-TPM-08	-0.42	0.07	-0.06	0.06	
BW-TPM-03	-0.65	0.07	0.03	0.06	1
BW-TPM-04	-0.38	0.07	0.06	0.06	
BE-TPM-09	-0.43	0.07	0.04	0.06	
BE-TPM-10	-0.45	0.07	0.02	0.06	
BE-TPM-12	-0.54	0.07	0.05	0.06	
DW-TPM-05	-0.35	0.07	0.07	0.06	
Sept-28-D	-0.48	0.06	0.02	0.04	
Sept-28-N	-0.46	0.06	0.01	0.04	4
Oct-5-D	-0.53	0.06	0.09	0.04	
Oct-5-N	-0.51	0.06	0.06	0.04	
Hg2-6, 2014	-0.34	0.07	-0.01	0.06	
Hg7, 2014	-0.42	0.07	-0.03	0.06	5
Hg8, 2014	-0.71	0.07	-0.01	0.06	
Hg9-13, 2014	-0.34	0.07	0.02	0.06	
ZSS-47	-0.32	N.A.	0.05	N.A.	
ZSS-48	-0.35	N.A.	-0.01	N.A.	
ZSS-51	-0.4	N.A.	-0.01	N.A.	
ZSS-52	-0.37	N.A.	-0.01	N.A.	
ZSS-53	-0.76	N.A.	-0.06	N.A.	
ZSS-54	-0.45	N.A.	-0.05	N.A.	
ZSS-55	-0.59	N.A.	-0.02	N.A.	
ZSS-56	-0.39	N.A.	-0.02	N.A.	
ZSS-57	-0.6	N.A.	-0.03	N.A.	
ZSS-58	-0.49	N.A.	-0.04	N.A.	
ZSS-61	-0.72	N.A.	-0.03	N.A.	
ZSS-62	-0.6	N.A.	-0.05	N.A.	
ZSS-64	-0.59	N.A.	0.03	N.A.	
ZSS-65	-0.47	N.A.	-0.09	N.A.	
ZSS-66	-0.32	N.A.	-0.01	N.A.	6
ZSS-68	-0.43	N.A.	-0.04	N.A.	
ZSS-75	-0.45	N.A.	0	N.A.	
ZSS-76	-0.41	N.A.	0.02	N.A.	
ZSS-77	-0.34	N.A.	-0.01	N.A.	
ZSS-79	-0.37	N.A.	-0.02	N.A.	
ZSS-81	-0.36	N.A.	-0.04	N.A.	
ZSS-82	-0.33	N.A.	-0.02	N.A.	
ZSS-84	-0.31	N.A.	0.08	N.A.	
ZSS-85	-0.5	N.A.	-0.04	N.A.	
ZSS-86	-0.37	N.A.	-0.04	N.A.	
ZSS-87	-0.4	N.A.	-0.04	N.A.	
ZSS-89	-0.37	N.A.	-0.09	N.A.	
ZSS-91	-0.37	N.A.	-0.05	N.A.	
ZSS-92	-0.36	N.A.	-0.05	N.A.	
16	-0.30	0.10	-0.02	0.05	this study

25	-0.27	0.09	-0.01	0.04	
26	-0.32	0.09	-0.10	0.04	
37	-0.31	0.12	-0.11	0.06	
mean	**-0.45**		**-0.01**		
sd	**0.14**		**0.05**		
PBM samples dominated by photoreduction					
MCB_PBM-35	0.85	0.09	0.09	0.08	
MCB_PBM-37	0.68	0.09	0.08	0.08	
MCB_PBM-38	0.66	0.09	0.08	0.08	
MCB_PBM-39	1.15	0.09	0.09	0.08	
MAL_PBM-3	0.82	0.09	0.09	0.08	7
MAL_PBM-13	0.86	0.09	0.05	0.08	
MAL_PBM-18	0.76	0.09	0.05	0.08	
MAL_PBM-20	1.07	0.09	0.08	0.08	
MAL_PBM-24	0.81	0.09	0.07	0.08	
HNI-PBM-16	0.68	0.09	0.06	0.08	
mean	**0.83**		**0.07**		
sd	**0.16**		**0.02**		
PBM samples dominated by troposphere photochemical reactions					
1	-0.29	0.04	1.24	0.08	
12	0.36	0.01	1.21	0.10	8
46	0.47	0.06	1.18	0.09	
mean	**0.18**		**1.21**		
sd	**0.41**		**0.03**		

N.A.: Not available.

Table S6 Estimated contribution of photoreduction based on the ratios of $\Delta^{199}Hg/\Delta^{200}Hg$ (k).

GEM*			PBM					
n	$\Delta^{199}Hg$ (‰)	$\Delta^{200}Hg$ (‰)	n	$\Delta^{199}Hg$ (‰)	$\Delta^{200}Hg$ (‰)	k	f_{red} (%)	altitudes/references
precipitation								
7	-0.09±0.09	-0.04±0.04	20	0.30±0.14	0.16±0.06	1.87	55	[9]
208	-0.20±0.08	-0.06±0.06	19	0.59±0.25	0.39±0.24	1.79	53	[8]
208	-0.20±0.08	-0.06±0.06	26	0.35±0.21	0.07±0.04	4.32	82	[10]
3	-0.19±0.03	-0.10±0.02	5	0.48±0.27	0.18±0.05	2.39	65	[11]
208	-0.20±0.08	-0.06±0.06	45	0.25±0.19	0.11±0.07	2.72	69	[12]
208	-0.20±0.08	-0.06±0.06	16	0.68±0.38	0.08±0.06	6.40	90	[13]
208	-0.20±0.08	-0.06±0.06	18	0.04±0.15	0.11±0.05	1.49	45	[1]
PBM collected in high latitudes								
208	-0.20±0.08	-0.06±0.06	7	-0.07±0.12	0.03±0.03	1.60	48	550 m[14]
208	-0.20±0.08	-0.06±0.06	21	0.35±0.34	0.08±0.04	4.17	82	50 m[7]
208	-0.20±0.08	-0.06±0.06	36	0.66±0.32	0.09±0.05	6.04	89	2450 m[7]
208	-0.20±0.08	-0.06±0.06	39	0.36±0.34	0.10±0.04	3.73	79	741 m[7]
208	-0.20±0.08	-0.06±0.06	25	0.27±0.22	0.07±0.03	3.89	80	3816 m[7]

* The mean GEM isotope compositions compiled from the literatures are used if there is no corresponding GEM isotope data reported in the references. The uncertainties are SD.

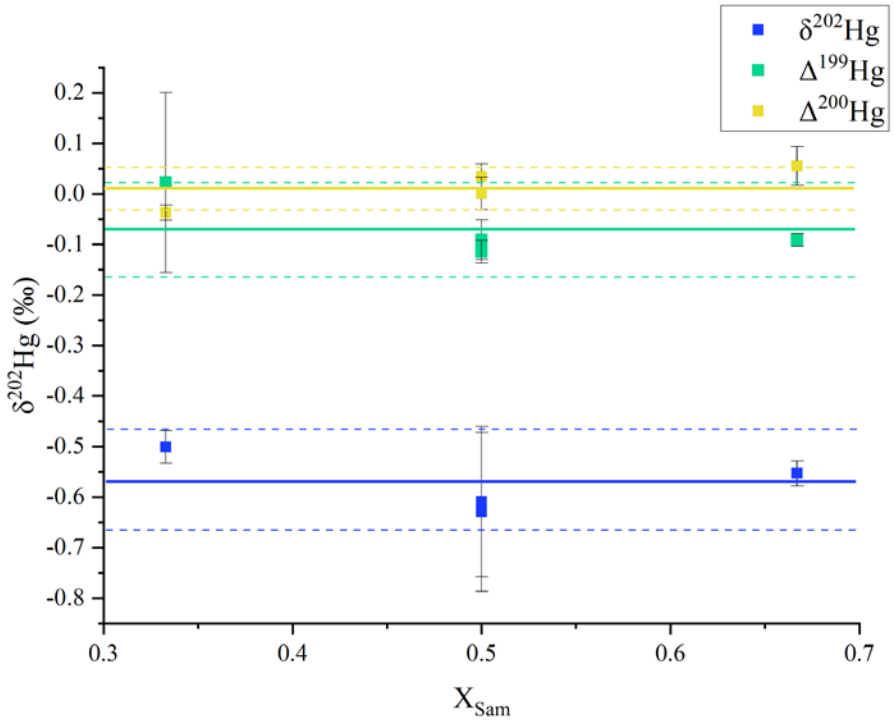

Figure S1. Calculated isotopic compositions of NIST 8610 when mixed with different proportions of NIST 3133. The bold and dashed lines represent the average and the ±1SD interval determined from all calculations, respectively.

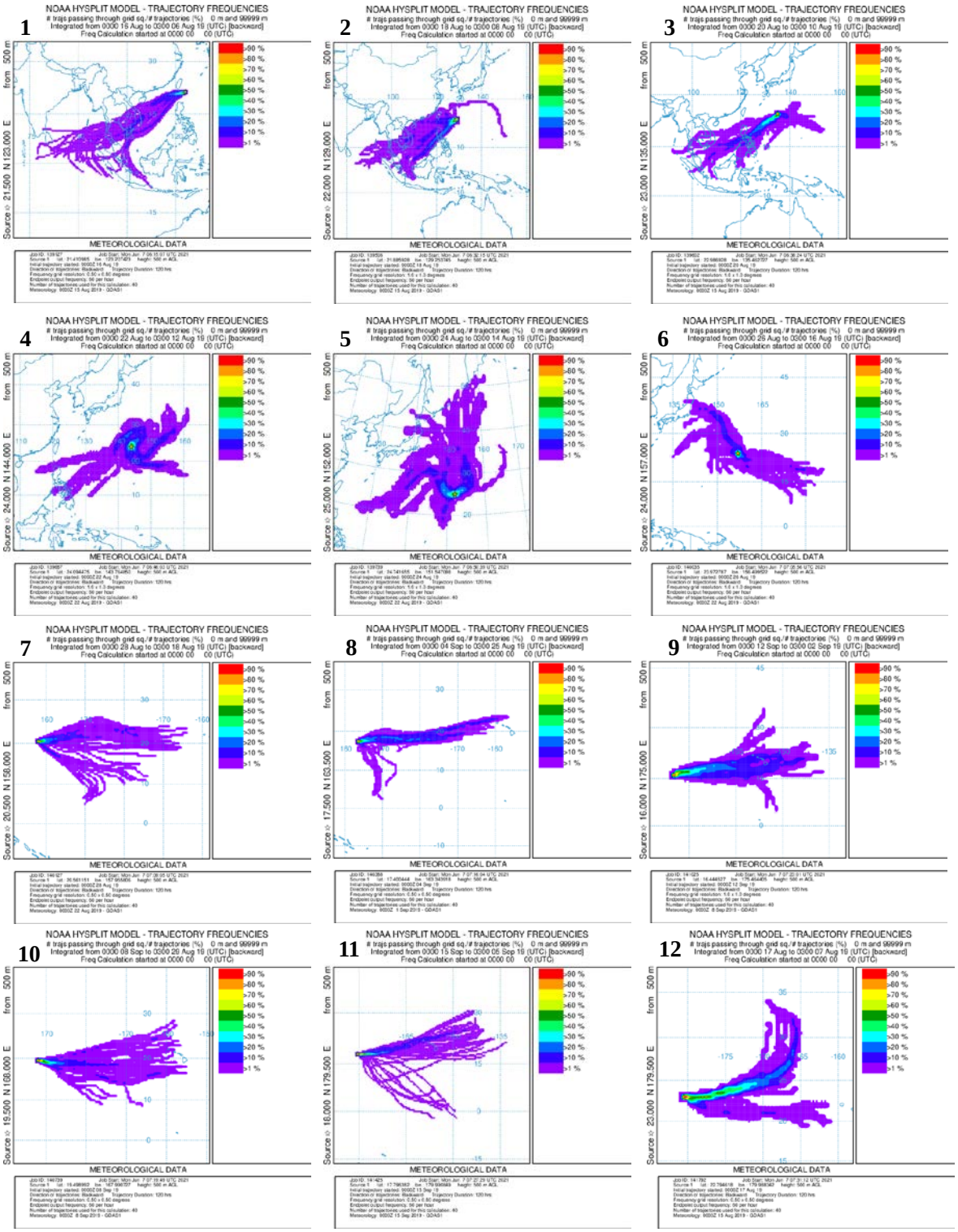
1
NOAA HYSPLIT MODEL - TRAJECTORY FREQUENCIES
trajs passing through grid sq./# trajectories (%) 0 m and 99999 m
Integrated from 0000 16 Aug to 0300 06 Aug 19 (UTC) [backward]
Freq Calculation started at 0000 00 00 (UTC)
Source 1 from 500 m
Source ☆ 21.500 N 123.000 E
METEOROLOGICAL DATA
2
NOAA HYSPLIT MODEL - TRAJECTORY FREQUENCIES
trajs passing through grid sq./# trajectories (%) 0 m and 99999 m
Integrated from 0000 19 Aug to 0300 08 Aug 19 (UTC) [backward]
Freq Calculation started at 0000 00 00 (UTC)
Source 1 from 500 m
Source ☆ 22.000 N 129.000 E
METEOROLOGICAL DATA
3
NOAA HYSPLIT MODEL - TRAJECTORY FREQUENCIES
trajs passing through grid sq./# trajectories (%) 0 m and 99999 m
Integrated from 0000 23 Aug to 0300 10 Aug 19 (UTC) [backward]
Freq Calculation started at 0000 00 00 (UTC)
Source 1 from 500 m
Source ☆ 20.000 N 135.000 E
METEOROLOGICAL DATA
4
NOAA HYSPLIT MODEL - TRAJECTORY FREQUENCIES
trajs passing through grid sq./# trajectories (%) 0 m and 99999 m
Integrated from 0000 22 Aug to 0300 12 Aug 19 (UTC) [backward]
Freq Calculation started at 0000 00 00 (UTC)
Source 1 from 500 m
Source ☆ 24.000 N 144.000 E
METEOROLOGICAL DATA
5
NOAA HYSPLIT MODEL - TRAJECTORY FREQUENCIES
trajs passing through grid sq./# trajectories (%) 0 m and 99999 m
Integrated from 0000 24 Aug to 0300 14 Aug 19 (UTC) [backward]
Freq Calculation started at 0000 00 00 (UTC)
Source 1 from 500 m
Source ☆ 25.000 N 152.000 E
METEOROLOGICAL DATA
6
NOAA HYSPLIT MODEL - TRAJECTORY FREQUENCIES
trajs passing through grid sq./# trajectories (%) 0 m and 99999 m
Integrated from 0000 26 Aug to 0300 16 Aug 19 (UTC) [backward]
Freq Calculation started at 0000 00 00 (UTC)
Source 1 from 500 m
Source ☆ 24.000 N 157.000 E
METEOROLOGICAL DATA
7
NOAA HYSPLIT MODEL - TRAJECTORY FREQUENCIES
trajs passing through grid sq./# trajectories (%) 0 m and 99999 m
Integrated from 0000 28 Aug to 0300 18 Aug 19 (UTC) [backward]
Freq Calculation started at 0000 00 00 (UTC)
Source 1 from 500 m
Source ☆ 20.500 N 156.000 E
METEOROLOGICAL DATA
8
NOAA HYSPLIT MODEL - TRAJECTORY FREQUENCIES
trajs passing through grid sq./# trajectories (%) 0 m and 99999 m
Integrated from 0000 04 Sep to 0000 25 Aug 19 (UTC) [backward]
Freq Calculation started at 0000 00 00 (UTC)
Source 1 from 500 m
Source ☆ 17.500 N 163.500 E
METEOROLOGICAL DATA
9
NOAA HYSPLIT MODEL - TRAJECTORY FREQUENCIES
trajs passing through grid sq./# trajectories (%) 0 m and 99999 m
Integrated from 0000 12 Sep to 0000 02 Sep 19 (UTC) [backward]
Freq Calculation started at 0000 00 00 (UTC)
Source 1 from 500 m
Source ☆ 16.000 N 175.000 E
METEOROLOGICAL DATA
10
NOAA HYSPLIT MODEL - TRAJECTORY FREQUENCIES
trajs passing through grid sq./# trajectories (%) 0 m and 99999 m
Integrated from 0000 08 Sep to 0000 26 Aug 19 (UTC) [backward]
Freq Calculation started at 0000 00 00 (UTC)
Source 1 from 500 m
Source ☆ 19.500 N 168.000 E
METEOROLOGICAL DATA
11
NOAA HYSPLIT MODEL - TRAJECTORY FREQUENCIES
trajs passing through grid sq./# trajectories (%) 0 m and 99999 m
Integrated from 0000 15 Sep to 0000 05 Sep 19 (UTC) [backward]
Freq Calculation started at 0000 00 00 (UTC)
Source 1 from 500 m
Source ☆ 16.000 N 179.500 E
METEOROLOGICAL DATA
12
NOAA HYSPLIT MODEL - TRAJECTORY FREQUENCIES
trajs passing through grid sq./# trajectories (%) 0 m and 99999 m
Integrated from 0000 17 Aug to 0000 07 Aug 19 (UTC) [backward]
Freq Calculation started at 0000 00 00 (UTC)
Source 1 from 500 m
Source ☆ 20.000 N 179.500 E
METEOROLOGICAL DATA

70

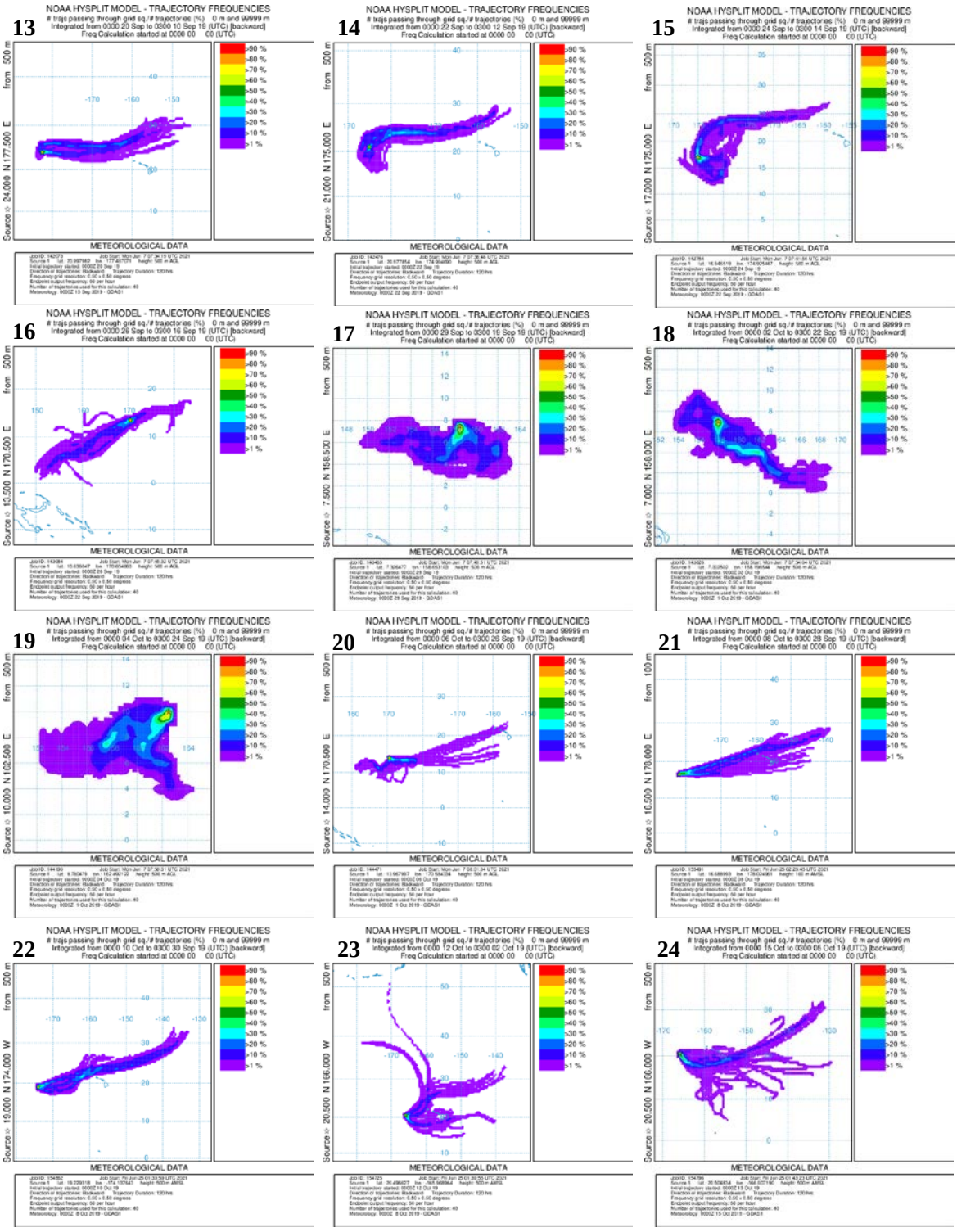
13
NOAA HYSPLIT MODEL - TRAJECTORY FREQUENCIES
14
NOAA HYSPLIT MODEL - TRAJECTORY FREQUENCIES
15
NOAA HYSPLIT MODEL - TRAJECTORY FREQUENCIES
16
NOAA HYSPLIT MODEL - TRAJECTORY FREQUENCIES
17
NOAA HYSPLIT MODEL - TRAJECTORY FREQUENCIES
18
NOAA HYSPLIT MODEL - TRAJECTORY FREQUENCIES
19
NOAA HYSPLIT MODEL - TRAJECTORY FREQUENCIES
20
NOAA HYSPLIT MODEL - TRAJECTORY FREQUENCIES
21
NOAA HYSPLIT MODEL - TRAJECTORY FREQUENCIES
22
NOAA HYSPLIT MODEL - TRAJECTORY FREQUENCIES
23
NOAA HYSPLIT MODEL - TRAJECTORY FREQUENCIES
24
NOAA HYSPLIT MODEL - TRAJECTORY FREQUENCIES
METEOROLOGICAL DATA

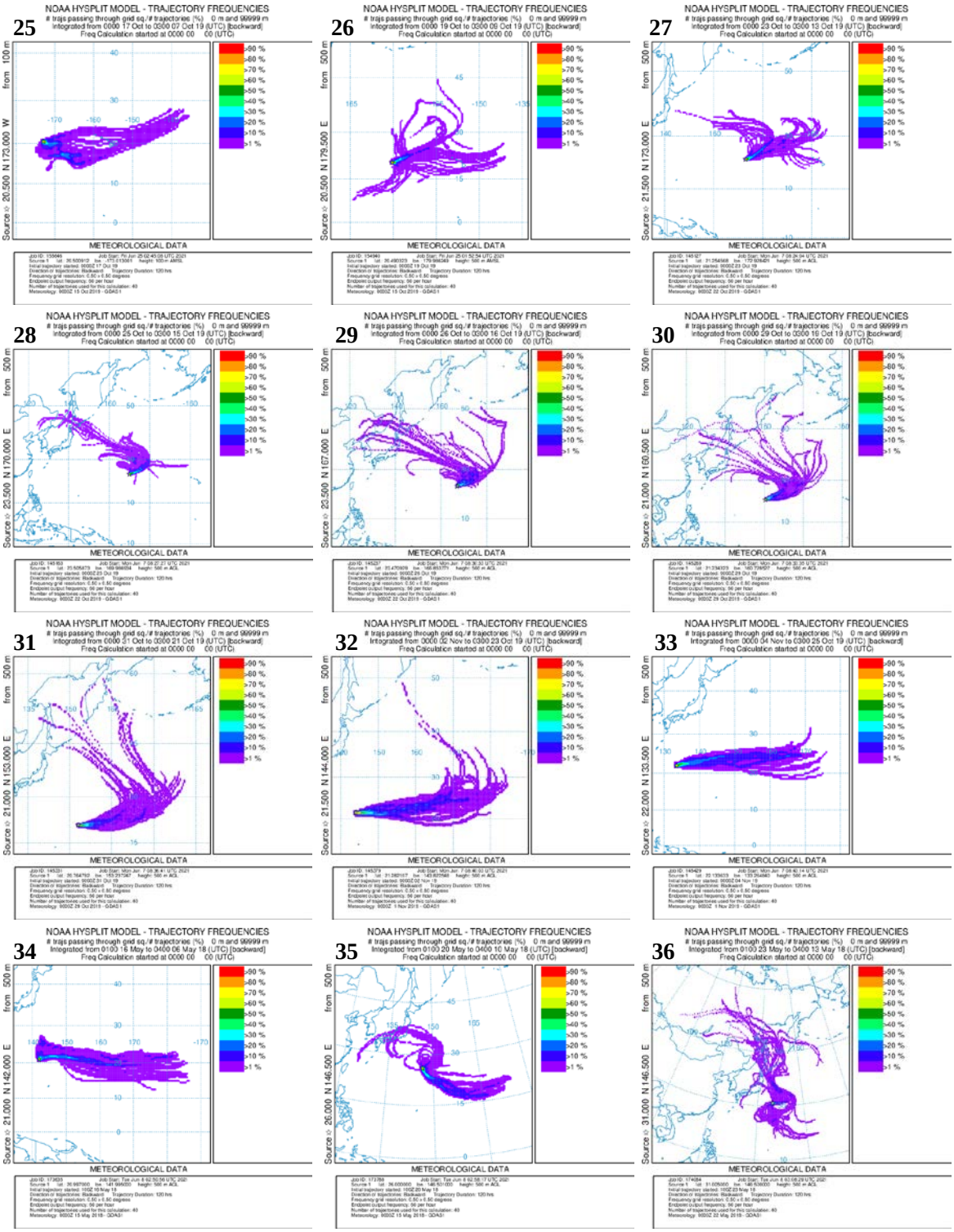
25
NOAA HYSPLIT MODEL - TRAJECTORY FREQUENCIES
trajs passing through grid sq./# trajectories (%) 0 m and 99999 m
Integrated from 0000 17 Oct to 0300 07 Oct 19 (UTC) [backward]
Freq Calculation started at 0000 00 00 (UTC)
Source ☆ 20.500 N 173.000 W from 100 m
METEOROLOGICAL DATA
26
NOAA HYSPLIT MODEL - TRAJECTORY FREQUENCIES
trajs passing through grid sq./# trajectories (%) 0 m and 99999 m
Integrated from 0000 19 Oct to 0300 09 Oct 19 (UTC) [backward]
Freq Calculation started at 0000 00 00 (UTC)
Source ☆ 20.500 N 179.500 E from 500 m
METEOROLOGICAL DATA
27
NOAA HYSPLIT MODEL - TRAJECTORY FREQUENCIES
trajs passing through grid sq./# trajectories (%) 0 m and 99999 m
Integrated from 0000 23 Oct to 0300 13 Oct 19 (UTC) [backward]
Freq Calculation started at 0000 00 00 (UTC)
Source ☆ 21.500 N 173.000 E from 500 m
METEOROLOGICAL DATA
28
NOAA HYSPLIT MODEL - TRAJECTORY FREQUENCIES
trajs passing through grid sq./# trajectories (%) 0 m and 99999 m
Integrated from 0000 25 Oct to 0300 15 Oct 19 (UTC) [backward]
Freq Calculation started at 0000 00 00 (UTC)
Source ☆ 23.500 N 170.000 E from 500 m
METEOROLOGICAL DATA
29
NOAA HYSPLIT MODEL - TRAJECTORY FREQUENCIES
trajs passing through grid sq./# trajectories (%) 0 m and 99999 m
Integrated from 0000 26 Oct to 0300 16 Oct 19 (UTC) [backward]
Freq Calculation started at 0000 00 00 (UTC)
Source ☆ 23.500 N 167.000 E from 500 m
METEOROLOGICAL DATA
30
NOAA HYSPLIT MODEL - TRAJECTORY FREQUENCIES
trajs passing through grid sq./# trajectories (%) 0 m and 99999 m
Integrated from 0000 29 Oct to 0300 19 Oct 19 (UTC) [backward]
Freq Calculation started at 0000 00 00 (UTC)
Source ☆ 21.000 N 160.500 E from 500 m
METEOROLOGICAL DATA
31
NOAA HYSPLIT MODEL - TRAJECTORY FREQUENCIES
trajs passing through grid sq./# trajectories (%) 0 m and 99999 m
Integrated from 0000 31 Oct to 0300 21 Oct 19 (UTC) [backward]
Freq Calculation started at 0000 00 00 (UTC)
Source ☆ 21.000 N 153.000 E from 500 m
METEOROLOGICAL DATA
32
NOAA HYSPLIT MODEL - TRAJECTORY FREQUENCIES
trajs passing through grid sq./# trajectories (%) 0 m and 99999 m
Integrated from 0000 02 Nov to 0300 23 Oct 19 (UTC) [backward]
Freq Calculation started at 0000 00 00 (UTC)
Source ☆ 21.500 N 144.000 E from 500 m
METEOROLOGICAL DATA
33
NOAA HYSPLIT MODEL - TRAJECTORY FREQUENCIES
trajs passing through grid sq./# trajectories (%) 0 m and 99999 m
Integrated from 0000 04 Nov to 0300 25 Oct 19 (UTC) [backward]
Freq Calculation started at 0000 00 00 (UTC)
Source ☆ 22.000 N 133.500 E from 500 m
METEOROLOGICAL DATA
34
NOAA HYSPLIT MODEL - TRAJECTORY FREQUENCIES
trajs passing through grid sq./# trajectories (%) 0 m and 99999 m
Integrated from 0100 16 May to 0400 06 May 18 (UTC) [backward]
Freq Calculation started at 0000 00 00 (UTC)
Source ☆ 21.000 N 142.000 E from 500 m
METEOROLOGICAL DATA
35
NOAA HYSPLIT MODEL - TRAJECTORY FREQUENCIES
trajs passing through grid sq./# trajectories (%) 0 m and 99999 m
Integrated from 0100 20 May to 0400 10 May 18 (UTC) [backward]
Freq Calculation started at 0000 00 00 (UTC)
Source ☆ 26.000 N 146.500 E from 500 m
METEOROLOGICAL DATA
36
NOAA HYSPLIT MODEL - TRAJECTORY FREQUENCIES
trajs passing through grid sq./# trajectories (%) 0 m and 99999 m
Integrated from 0100 23 May to 0400 13 May 18 (UTC) [backward]
Freq Calculation started at 0000 00 00 (UTC)
Source ☆ 31.000 N 146.500 E from 500 m
METEOROLOGICAL DATA

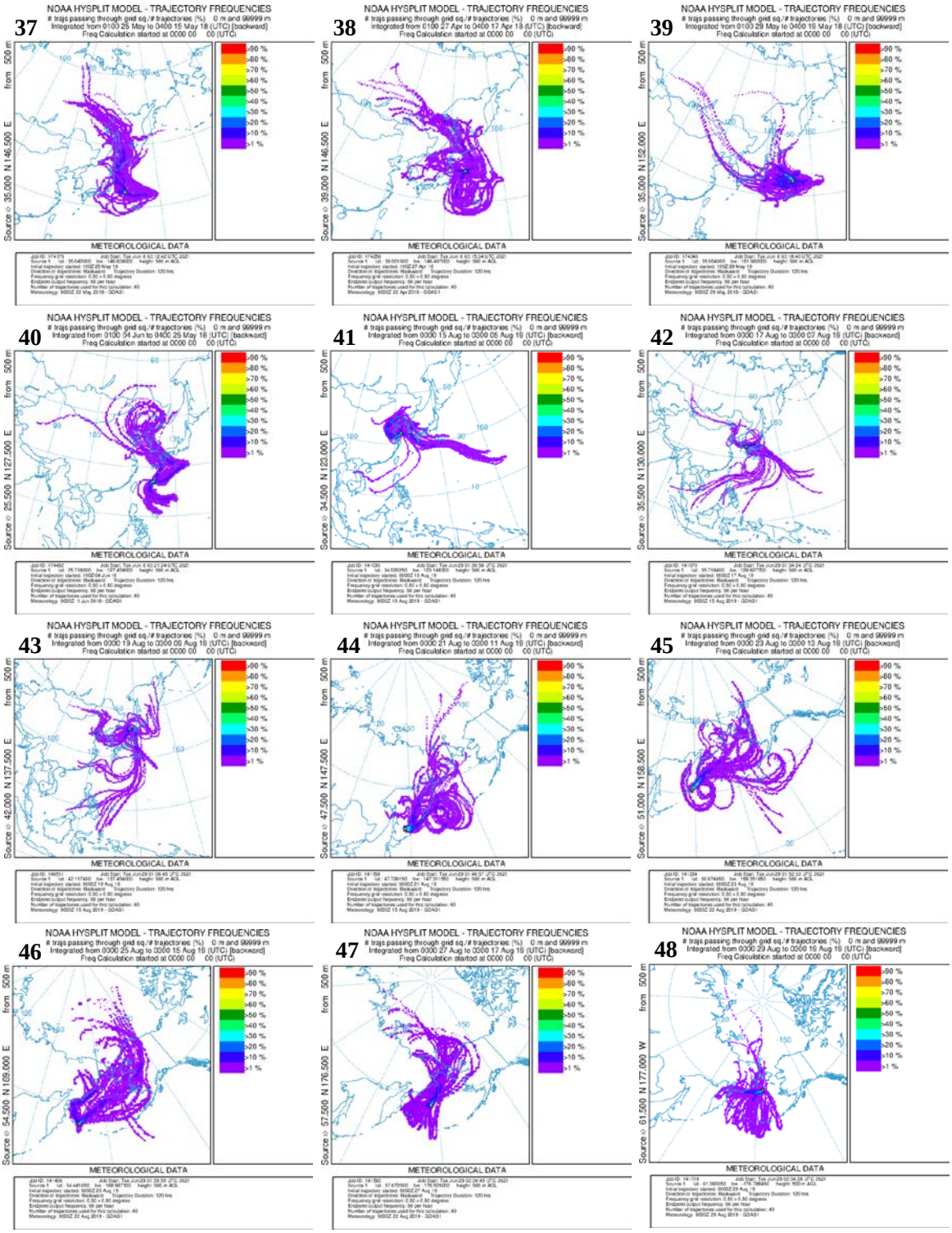
37
NOAA HYSPLIT MODEL - TRAJECTORY FREQUENCIES
38
NOAA HYSPLIT MODEL - TRAJECTORY FREQUENCIES
39
NOAA HYSPLIT MODEL - TRAJECTORY FREQUENCIES
40
NOAA HYSPLIT MODEL - TRAJECTORY FREQUENCIES
41
NOAA HYSPLIT MODEL - TRAJECTORY FREQUENCIES
42
NOAA HYSPLIT MODEL - TRAJECTORY FREQUENCIES
43
NOAA HYSPLIT MODEL - TRAJECTORY FREQUENCIES
44
NOAA HYSPLIT MODEL - TRAJECTORY FREQUENCIES
45
NOAA HYSPLIT MODEL - TRAJECTORY FREQUENCIES
46
NOAA HYSPLIT MODEL - TRAJECTORY FREQUENCIES
47
NOAA HYSPLIT MODEL - TRAJECTORY FREQUENCIES
48
NOAA HYSPLIT MODEL - TRAJECTORY FREQUENCIES
METEOROLOGICAL DATA

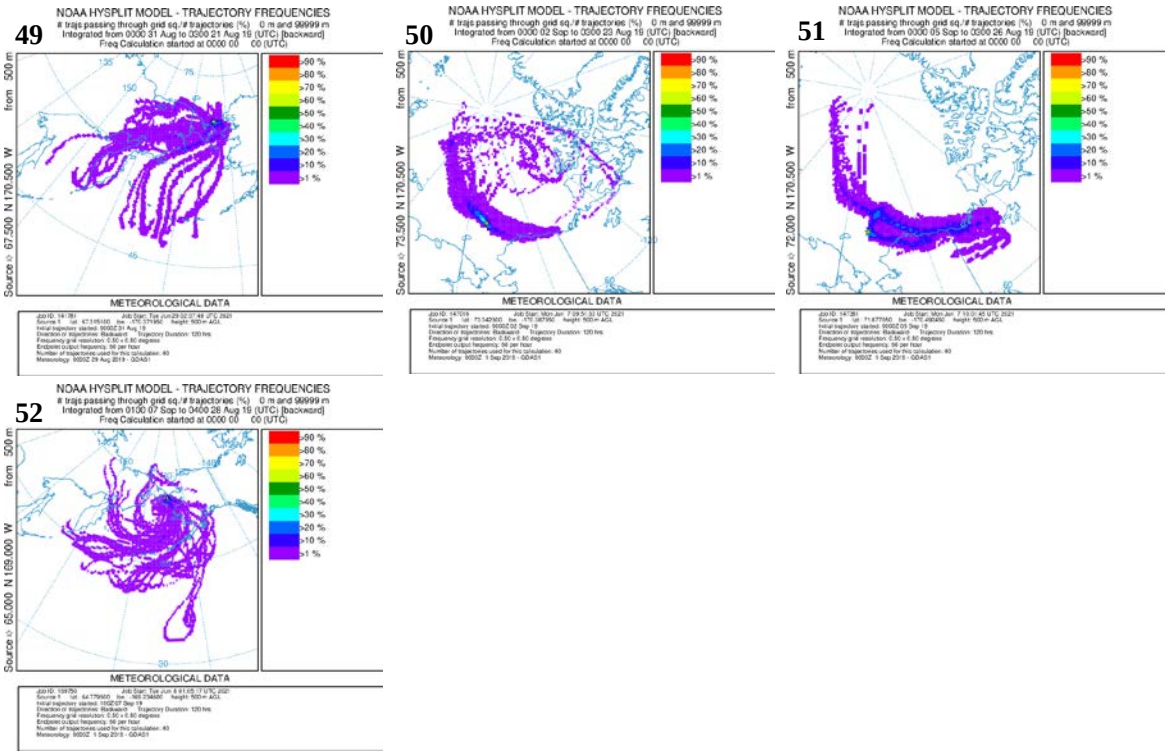

Figure S2. Trajectory frequency analysis showing the air mass arriving at each sampling site. Number in the top left represents sample ID.

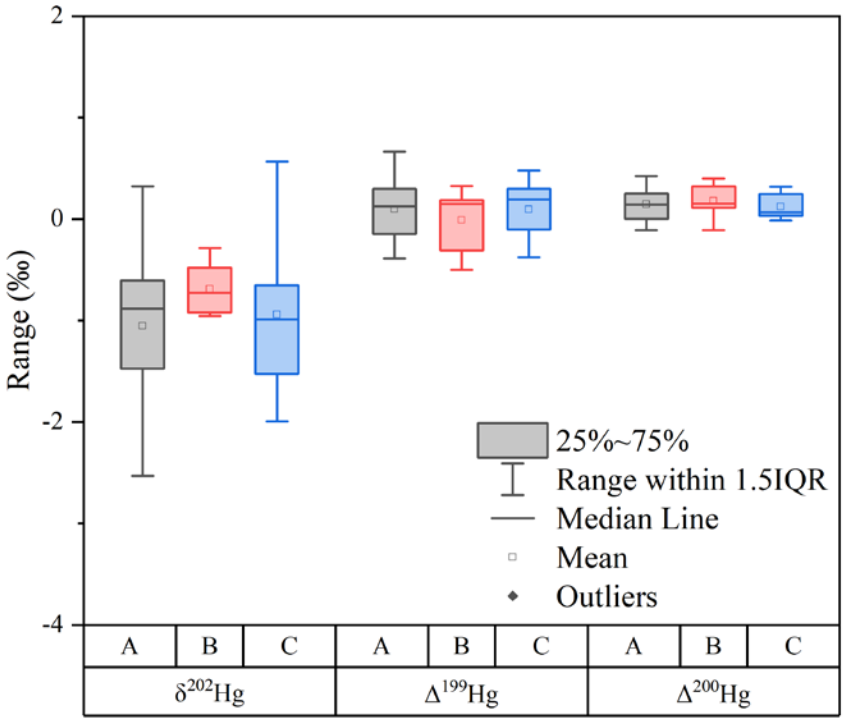

Figure S3. Box chart of PBM isotope signatures between different cruises.

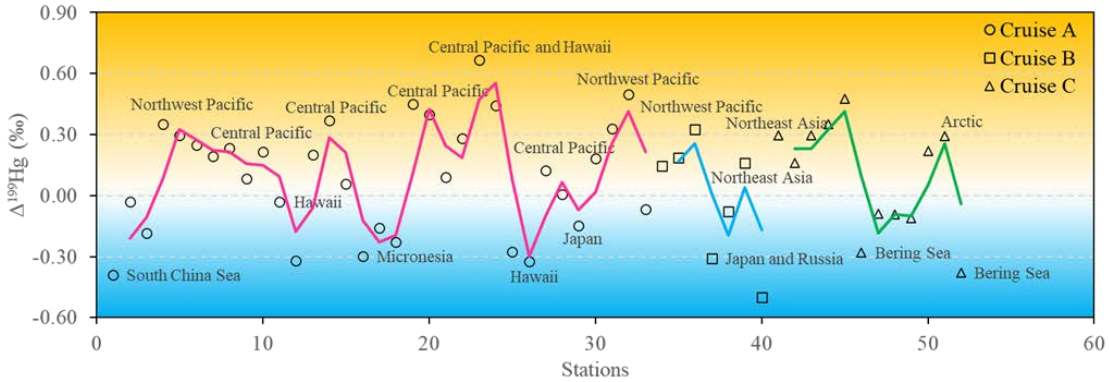

Figure S4. Variation in $\Delta^{199}Hg$ values of PBM during the three cruises. The annotation behind the point represents the potential source of the air mass at the station during sampling.

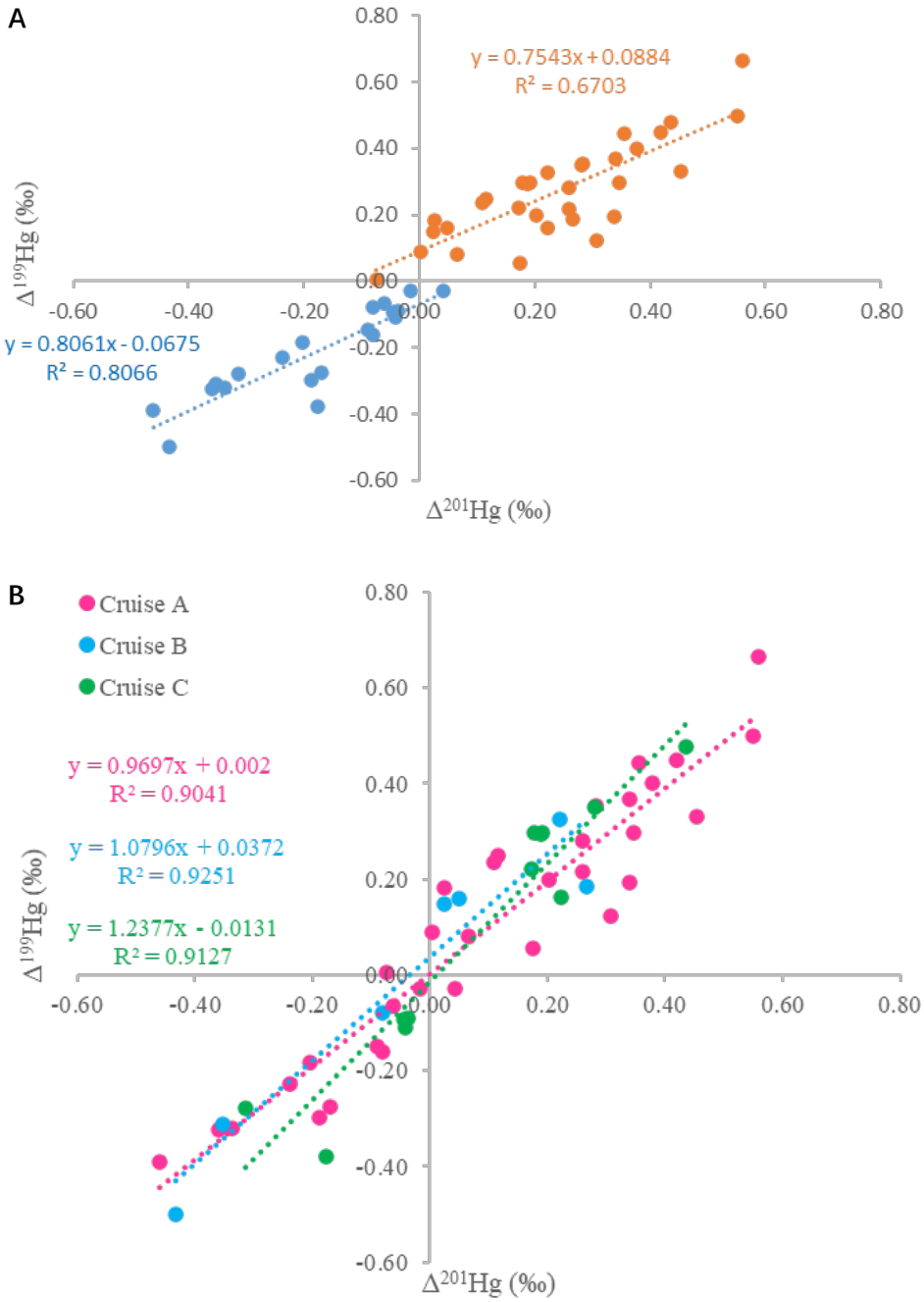

Figure S5. Plots of Δ^{199}Hg vs. Δ^{201}Hg for PBM with (A) positive and negative Δ^{199}Hg values and (B) different cruises.

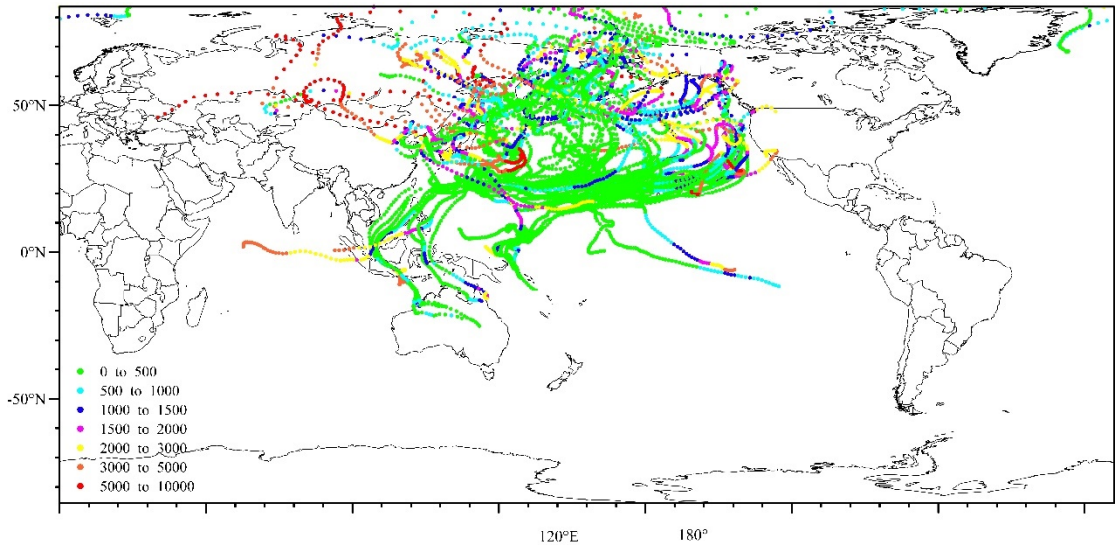

Figure S6. HYSPLIT trajectory analyses for each sampling sites in 13 days with overlap. Points of trajectories were calculated every 4 h.

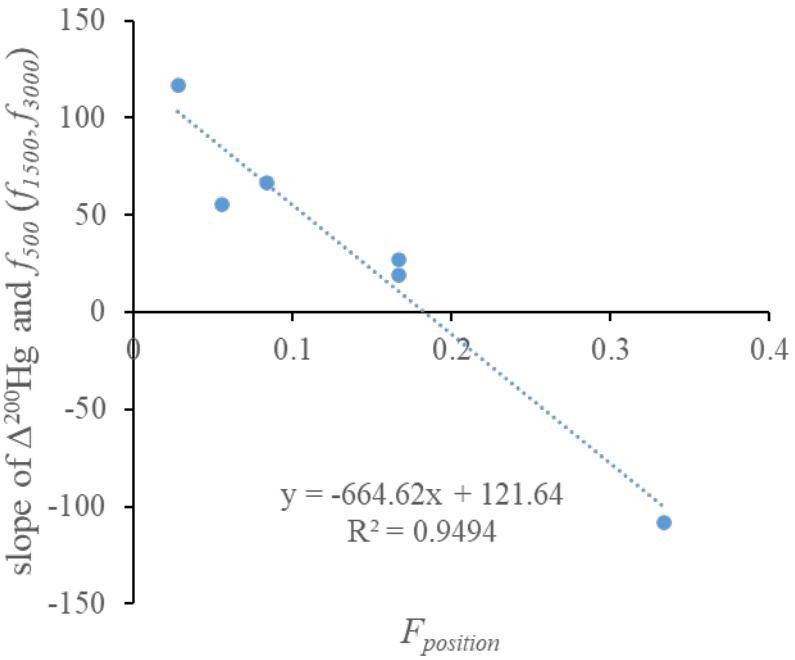

Figure S7. The relationship between Δ^{200}Hg and altitudes. This is shown as the slope of Δ^{200}Hg and f_{500} (f_{1500}, f_{3000}) versus F_{position}. F_{position} = height/9000 at high latitudes (Cruise B and C) and F_{position} = height/18000 at low latitudes (Cruise A), respectively. The slope is the ratios of f_{500}/Δ^{200}Hg, f_{1500}/Δ^{200}Hg, and f_{3000}/Δ^{200}Hg, as shown in Figure 6.

References:

1 Huang, S. *et al.* Natural stable isotopic compositions of mercury in aerosols and wet precipitations around a coal-fired power plant in Xiamen, southeast China. *Atmos. Environ.* **173**, 72-80 (2018).

2 Huang, S. *et al.* Application of an isotope binary mixing model for determination of precise mercury isotopic composition in samples with low mercury concentration. *Anal. Chem.* **91**, 7063-7069 (2019).

3 Qiu, Y. *et al.* Identification of potential sources of elevated PM2.5-Hg using mercury isotopes during haze events. *Atmos. Environ.* **247**, 118203, doi:10.1016/j.atmosenv.2021.118203 (2021).

4 Huang, Q. *et al.* Diel variation of mercury stable isotope ratios record photoreduction of PM2.5-bound mercury. *Atmos. Chem. Phys.*, 315-325 (2019).

5 Zheng, W. *et al.* Mercury stable isotopes reveal the sources and transformations of atmospheric Hg in the high Arctic. *Appl. Geochem.* **131**, 105002, doi:10.1016/j.apgeochem.2021.105002 (2021).

6 Li, C. *et al.* Seasonal Variation of Mercury and Its Isotopes in Atmospheric Particles at the Coastal Zhongshan Station, Eastern Antarctica. *Environ Sci Technol* **54**, 11344-11355, doi:10.1021/acs.est.0c04462 (2020).

7 Fu, X. *et al.* Domestic and Transboundary Sources of Atmospheric Particulate Bound Mercury in Remote Areas of China: Evidence from Mercury Isotopes. *Environ. Sci. Technol.* **53**, 1947-1957 (2019).

8 Chen, J., Hintelmann, H., Feng, X. & Dimock, B. Unusual fractionation of both odd and even mercury isotopes in precipitation from Peterborough, ON, Canada. *Geochim. Cosmochim. Acta* **90**, 33-46 (2012).

9 Gratz, L., Keeler, G., Blum, J. & Sherman, L. Isotopic Composition and Fractionation of Mercury in Great Lakes Precipitation and Ambient Air. *Environ. Sci. Technol.* **44**, 7770 (2010).

10 Yuan, S. *et al.* Sequential samples reveal significant variation of mercury isotope ratios during single rainfall events. *Sci. Total Environ.* **624**, 133-144 (2018).

11 Demers, J., Blum, J. & Zak, D. Mercury isotopes in a forested ecosystem: Implications for air-surface exchange dynamics and the global mercury cycle. *Global Biogeochem. Cycles* **27**, 222-238 (2013).

12 Sherman, L., Blum, J., Keeler, G., Demers, J. & Dvonch, J. Investigation of Local Mercury Deposition from a Coal-Fired Power Plant Using Mercury Isotopes. *Environ. Sci. Technol.* **46**, 382-390 (2012).

13 Wang, Z. *et al.* Mass-dependent and mass-independent fractionation of mercury isotopes in precipitation from Guiyang, SW China. *C.R. Geosci.* **347**, 358-367 (2015).

14 Yu, B. *et al.* Isotopic Composition of Atmospheric Mercury in China: New Evidence for Sources and Transformation Processes in Air and in Vegetation. *Environ. Sci. Technol.* **50**, 9262-9269 (2016).